magnetochemistry

MDPI

Article

Predicting Pt-195 NMR Chemical Shift and $^{1}J(^{195}Pt\text{-}^{31}P)$ Coupling Constant for Pt(0) Complexes Using the NMR-DKH Basis Sets

Joyce H. C. e Silva [1], Hélio F. Dos Santos [2] and Diego F. S. Paschoal [1,*]

[1] NQTCM—Núcleo de Química Teórica e Computacional de Macaé, Polo Ajuda, Instituto Multidisciplinar de Química, Centro Multidisciplinar UFRJ-Macaé, Universidade Federal do Rio de Janeiro, Macaé 27973-545, RJ, Brazil; joycecunha37@gmail.com

[2] NEQC—Núcleo de Estudos em Química Computacional, Departamento de Química-ICE, Universidade Federal de Juiz de Fora, Campus Universitário, Juiz de Fora 36036-900, MG, Brazil; helio.santos@ufjf.edu.br

* Correspondence: diegopaschoal01@gmail.com or diegofspaschoal@macae.ufrj.br

Abstract: Pt(0) complexes have been widely used as catalysts for important reactions, such as the hydrosilylation of olefins. In this context, nuclear magnetic resonance (NMR) spectroscopy plays an important role in characterising of new structures and elucidating reaction mechanisms. In particular, the Pt-195 NMR is fundamental, as it is very sensitive to the ligand type and the oxidation state of the metal. In the present study, quantum mechanics computational schemes are proposed for the theoretical prediction of the Pt-195 NMR chemical shift and $^{1}J(^{195}Pt–^{31}P)$ in Pt(0) complexes. The protocols were constructed using the B3LYP/LANL2DZ/def2-SVP/IEF-PCM(UFF) level for geometry optimization and the GIAO-PBE/NMR-DKH/IEF-PCM(UFF) level for NMR calculation. The NMR fundamental quantities were then scaled by empirical procedures using linear correlations. For a set of 30 Pt(0) complexes, the results showed a mean absolute deviation (MAD) and mean relative deviation (MRD) of only 107 ppm and 2.3%, respectively, for the Pt-195 NMR chemical shift. When the coupling constant is taken into account, the MAD and MRD for a set of 33 coupling constants in 26 Pt(0) complexes were of 127 Hz and 3.3%, respectively. In addition, the models were validated for a group of 17 Pt(0) complexes not included in the original group that had MAD/MRD of 92 ppm/1.7% for the Pt-195 NMR chemical shift and 146 Hz/3.6% for the $^{1}J(^{195}Pt–^{31}P)$.

Keywords: Pt(0) complexes; catalysis; NMR; Pt-195 chemical shift; basis set; DFT

Citation: e Silva, J.H.C.; Dos Santos, H.F.; Paschoal, D.F.S. Predicting Pt-195 NMR Chemical Shift and $^{1}J(^{195}Pt\text{-}^{31}P)$ Coupling Constant for Pt(0) Complexes Using the NMR-DKH Basis Sets. *Magnetochemistry* **2021**, *7*, 148. https://doi.org/10.3390/magnetochemistry7110148

Academic Editor: Alessandro Lunghi

Received: 20 September 2021
Accepted: 2 November 2021
Published: 12 November 2021

1. Introduction

Currently, there is a great interest in the study of Pt compounds due to their application as anticancer drugs [1,2] and due to their use as heterogeneous or homogeneous catalysts [3] in modern organic chemistry [4,5]. In particular, Pt(0) complexes are widely used as catalysts in hydrosilylation processes [6–10].

The Pt(0) complexes have coordination numbers (C.N.) 2, 3, and 4 and exhibit linear, trigonal, and tetrahedral geometries, respectively [11,12]. Considering the importance of Pt(0) complexes and their structural diversity, the nuclear magnetic resonance (NMR) spectroscopy for the Pt-195 nucleus is an important tool used for mechanistic studies [13]. Pt-195 NMR can help in structural characterization of the complexes, cis/trans discrimination, stoichiometry, elucidation of reaction mechanisms, etc. [11–13].

The studies on NMR of Pt-195 date back to the 1960s, when the effect of structure on the Pt chemical shift was first described [14]. The Pt-195 nucleus is the only active isotope of Pt with spin quantum number $I = \frac{1}{2}$, a relative sensitivity of 9.94×10^{-3} (^{1}H: 1.00), a gyromagnetic ratio $\gamma = 5.768 \times 10^{7}$ rad s^{-1} T^{-1}, and a natural abundance of 33.8% [13,15]. The Pt-195 NMR chemical shift ($\delta^{195}Pt$) includes values in the range of about 15,000 ppm, from +8000 to −7000 ppm relative to the reference compound $[PtCl_6]^{2-}$ in D_2O, which are sensitive to the oxidation state of Pt (0, 2, or 4), temperature, solvent, type of ligands in the

coordination sphere, and their spatial arrangement [11,13–15]. In addition, the one-bond spin–spin coupling constant (SSCC) $^{1}J^{195}$Pt–L (L = Ligand) provides important information about the spatial position of the ligands [15].

Theoretical prediction of Pt-195 NMR parameters is a difficult task, as several factors must be taken into account, such as the geometry of the complexes, electronic correlation, basis sets, solvents, and relativistic effects [16–20]. Despite this difficulty, some works on the theoretical prediction of δ^{195}Pt and $^{1}J^{195}$Pt–L for Pt(II) and Pt(IV) complexes can be found in the literature [18–26]. However, computational studies on NMR prediction of Pt-195 in Pt(0) complexes are still very scarce [27].

In a previous paper [18], we developed an all-electron relativistic triple-zeta doubly polarized basis set (NMR-DKH) for Pt and the main ligand atoms. In addition, an empirical model for predicting Pt-195 NMR chemical shift in Pt(II) complexes was proposed. For a set of 258 Pt(II) complexes, a mean absolute deviation (MAD) and mean relative deviation (MRD) of 168 ppm and 5%, respectively, were obtained at GIAO-PBE/NMR-DKH/IEF-PCM(UFF)//B3LYP/LANL2DZ/def2-SVP/IEF-PCM(UFF) level (double slashes mean that the NMR properties were calculated at GIAO-PBE/NMR-DKH/IEF-PCM(UFF) and the structure at B3LYP/LANL2DZ/def2-SVP/IEF-PCM(UFF)), followed by an empirical scaling procedure. Then, the same computational protocol as in Ref. [18] was used to build an empirical model for predicting $^{1}J(^{195}Pt–^{15}N)$ for a set of 71 Pt(II) complexes, which yielded a MAD of 36 Hz and an MRD of 10.4% [19]. In the present work, we extend our previous studies by proposing quantum mechanical computational schemes to predict Pt-195 NMR chemical shift and $^{1}J(^{195}Pt–^{31}P)$ for Pt(0) complexes.

2. Theoretical Methodology

The geometries of all Pt(0) complexes (see Supplementary Materials) studied in the present paper were optimized and characterized as a local minimum on the potential energy surface (PES) by the positive (real) values of all harmonic mode frequencies at density functional theory (DFT) level with the hybrid functional B3LYP [28–30], the effective core potential (ECP) LANL2DZ [31,32] for Pt and the def2-SVP [33] basis set for ligands atoms (B3LYP/LANL2DZ/def2-SVP/IEF-PCM(UFF)). The solvent effect was considered in both geometry optimization and NMR calculations using the integral equation formalism for polarized continuum method (IEF-PCM) and the radii were set as for UFF force field [34]. For each Pt(0) complex, the solvent considered in the calculations is the same as used in the experimental measurements. All Pt(0) complexes studied in the present paper have a singlet electronic ground state [12].

The Pt-195 NMR shielding constant (σ^{195}Pt) and the $^{1}J(^{195}Pt–^{31}P)$ were calculated from the gauge-independent atomic orbitals (GIAO) [35,36] method at DFT level using the GGA PBE [37] functional with the NMR-DKH [18] basis sets (GIAO-PBE/NMR-DKH/IEF-PCM(UFF)). The computational protocol (NMR/geometry) is represented as in our previous papers [18,19], namely, GIAO-PBE/NMR-DKH/IEF-PCM(UFF)//B3LYP/LANL2DZ/def2-SVP/IEF-PCM(UFF). All calculations were carried out in the GAUSSIAN 09 program Revision D.01 [38].

The NMR fundamental quantities, σ^{195}Pt and the $^{1}J(^{195}Pt–^{31}P)$, were used as independent variables to fit the scaling models. The Equation (1) was used to predict δ^{195}Pt, in which the "a" and "b" parameters were fitted using a standard linear correlation for a set of 30 Pt(0) complexes for which experimental data are found in the literature.

$$\delta^{195}\mathrm{Pt}_{\mathrm{calc.}} = \mathrm{a} \times \sigma^{195}\mathrm{Pt}_{\mathrm{calc.}} + \mathrm{b} \quad (1)$$

For $^{1}J(^{195}Pt–^{31}P)$, the Equation (2) was adjusted considering a set of 33 coupling constants in 26 Pt(0) complexes.

$$^{1}\mathrm{J}^{\mathrm{scal.}}\left(^{195}\mathrm{Pt} - ^{31}\mathrm{P}\right) = \mathrm{a} \times {}^{1}\mathrm{J}^{\mathrm{calc.}}\left(^{195}\mathrm{Pt} - ^{31}\mathrm{P}\right) + \mathrm{b} \quad (2)$$

In the last part, we validated the proposed scaling models using a set of 17 Pt(0) complexes not included in the original set.

3. Results and Discussion

As shown in our previous papers [18–20], the inclusion of relativistic effects is fundamental for the theoretical prediction of NMR parameters of the heavy Pt-195 nucleus. Relativistic Hamiltonians are not always available in computational packages, so the construction of nonrelativistic computational protocols must be of great interest and useful if properly scaled. In the present work, we present computational protocols using a nonrelativistic Hamiltonian for predicting δ^{195}Pt and $^{1}J(^{195}Pt–^{31}P)$ in Pt(0) complexes.

First, we discuss the Pt-195 NMR chemical shift for the Pt(0) complexes. To partially recover the relativistic effects and account for the intrinsic errors of the computational methods, an empirical scaling model (Equation (1)) was constructed from the linear correlation of the calculated σ^{195}Pt and the experimental δ^{195}Pt for a set of 30 Pt(0) complexes showing coordination numbers 2 and 3. The linear regression is shown in Figure 1a and the parameters a and b are given in Table 1 (Model 1). It can be observed that the obtained angular coefficient (a = −0.8277) is close to −1, indicating that the proposed empirical Model 1 is physically consistent [18]. Moreover, the coefficient of determination (R^2) was 0.95, which confirms the quality of the proposed empirical statistical model.

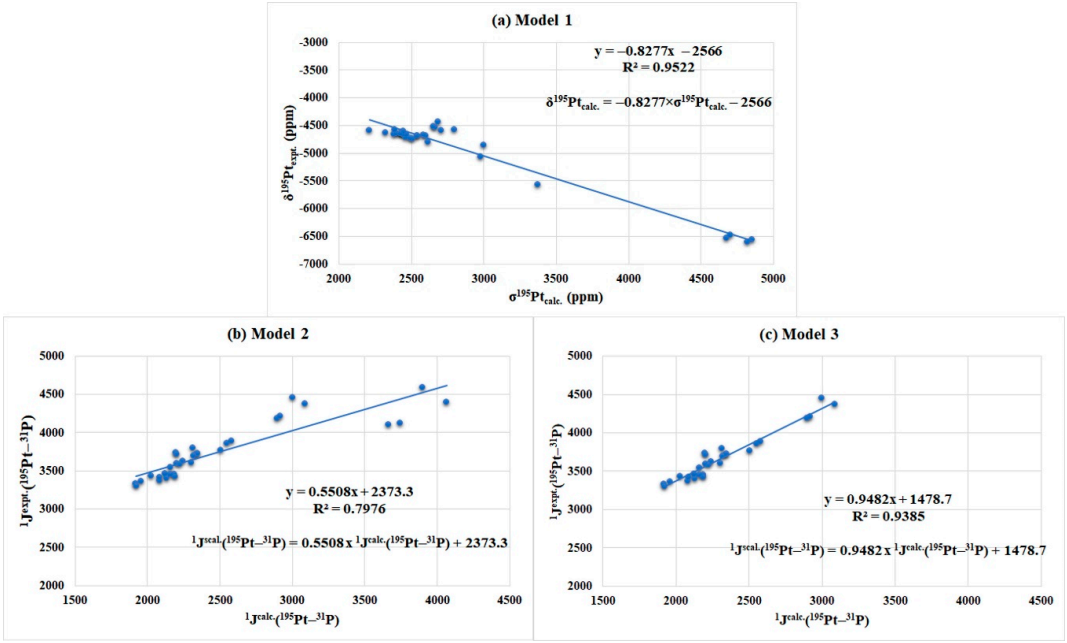

Figure 1. Linear regression between: (**a**) calculated σ^{195}Pt and experimental δ^{195}Pt for a set of 30 Pt(0) complexes (Model 1); (**b**) calculated and experimental $^{1}J(^{195}Pt–^{31}P)$ for a set of 33 coupling constants in 26 linear and trigonal-planar Pt(0) complexes (Model 2); and (**c**) calculated and experimental $^{1}J(^{195}Pt–^{31}P)$ for a set of 29 coupling constants in 22 trigonal-planar Pt(0) complexes (Model 3).

Table 1. Empirical scaling models obtained to predict δ^{195}Pt and $^{1}J(^{195}Pt–^{31}P)$ in Pt(0) complexes.

Models	Linear Regression Models	R^2
Model 1 [a]	$\delta^{195}Pt_{calc} = -0.8277 \times \sigma^{195}Pt_{calc} - 2566$	0.9522
Model 2 [b]	$^{1}J^{scal.}(^{195}Pt - ^{31}P) = 0.5508 \times {}^{1}J^{calc.}(^{195}Pt - ^{31}P) + 2373.3$	0.7976
Model 3 [c]	$^{1}J^{scal.}(^{195}Pt - ^{31}P) = 0.9482 \times {}^{1}J^{calc.}(^{195}Pt - ^{31}P) + 1478.7$	0.9385

[a] Model 1 constructed for linear (C.N. = 2) and trigonal (C.N. = 3) Pt(0) complexes using a set of 30 complexes. [b] Model 2 constructed for linear (C.N. = 2) and trigonal (C.N. = 3) Pt(0) complexes using a set of 33 coupling constant in 26 complexes. [c] Model 3 constructed for trigonal (C.N. = 3) Pt(0) complexes using a set of 29 coupling constant in 22 complexes. The fundamental quantities, δ^{195}Pt, and $^{1}J(^{195}Pt–^{31}P)$, were calculated at GIAO-PBE/NMR-DKH/IEF-PCM(UFF)//B3LYP/LANL2DZ/def2-SVP/IEF-PCM(UFF) level.

Table 2 shows the predicted Pt-195 NMR chemical shift using Model 1 for the 30 Pt(0) complexes. Considering all the complexes, the MAD and MRD were 107 ppm and 2.3%, respectively, showing that Model 1 has satisfactory predictive power. When the complexes with C.N. 2 and 3 are evaluated separately, the MAD and the MRD are 48 ppm and 0.7% (four linear complexes with C.N. 2), and 120 ppm and 2.6% (25 trigonal complexes with C.N. 3).

Table 2. Calculated δ^{195}Pt, in ppm, and $^{1}J(^{195}Pt–^{31}P)$, in Hz, for the Pt(0) complexes used in the construction of the proposed empirical models.

			δ^{195}Pt (ppm)		$^{1}J(^{195}Pt–^{31}P)$ (Hz)			
	Pt(0) Complexes	**Solvent**	**Model 1**	**Expt.**	**Model 0**	**Model 2**	**Model 3**	**Expt.**
	Linear Geometry (C.N. = 2)							
1	$[Pt(PPr^{i}_{3})_2]$	Toluene	−6557	−6607 [a]	3665	4392	-	4104 [b]
2	$[Pt(Pcy_3)_2]$, cy = cyclohexil	Toluene	−6583	−6555 [a]	3742	4435	-	4120 [b]
3	$[Pt(PBu^{t}_{2}Ph)_2$	Toluene	−6434	−6526 [a]	3898	4520	-	4592 [b]
4	$[Pt(PBu^{t}_{3})_2$	$THF\text{-}d_8$	−6457	−6479 [c]	4065	4612	-	4399 [c]
	MAD/MRD (C.N. = 2)		48/0.7%		461/11%	222/5.3%	-	
	Trigonal Geometry (C.N. = 3)							
5	$[Pt(PEt_3)_3]$	Toluene	−4768	−4526 [a]	2897	3969	4226	4188 [b]
6	$[Pt(PBu^{n}_{3})_3]$	Toluene	−4761	−4511 [a]	2916	3980	4244	4211 [b]
7	$[Pt(P(CH_2Ph)_3)_3]$	Toluene	−4790	−4439 [a]	3086	4073	4405	4377 [b]
8	$[Pt(Pcy_3)_3]$, cy = cyclohexil	Toluene	−4878	−4567 [a]	-	-	-	-
9	$[Pt(PPh_3)_2(PhCy{\equiv}CPh)]$	CD_2Cl_2	−4642	−4741 [d]	2186	3577	3551	3452 [d]
10	$[Pt(PPh_3)_2(PhC{\equiv}CMe)]$	CD_2Cl_2	−4630	−4727 [d]	2083	3520	3454	3377 [d]
			-	-	2159	3562	3526	3454 [d]
11	$[Pt(PPh_3)_2(PhC{\equiv}CCO_2Me)]$	CD_2Cl_2	−4602	−4710 [d]	2130	3547	3499	3403 [d]
			-	-	2196	3583	3561	3741 [d]
12	$[Pt(PPh_3)_2(PhC{\equiv}CH)]$	CD_2Cl_2	−4668	−4690 [d]	2121	3541	3490	3464 [d]
			-	-	2158	3562	3525	3547 [d]
13	$[Pt(PPh_3)_2(EtC{\equiv}CEt)]$	CD_2Cl_2	−4669	−4689 [d]	2189	3579	3554	3425 [d]
14	$[Pt(PPh_3)_2(MeC{\equiv}CCO_2Me)]$	CD_2Cl_2	−4719	−4682 [d]	1957	3451	3334	3366 [d]
			-	-	2312	3647	3671	3803 [d]
15	$[Pt(PPh_3)_2(MeC{\equiv}CMe)]$	CD_2Cl_2	−4702	−4674 [d]	2086	3522	3457	3420 [d]
16	$[Pt(PPh_3)_2(HC{\equiv}CH)]$	CD_2Cl_2	−4607	−4658 [d]	2242	3608	3604	3626 [d]
17	$[Pt(PPh_3)_2(EtO_2CC{\equiv}CCO_2Et)]$	CD_2Cl_2	−4586	−4655 [d]	2203	3587	3567	3722 [d]
18	$[Pt(PPh_3)_2(MeO_2CC{\equiv}CCO_2Me)]$	CD_2Cl_2	−4537	−4653 [d]	2342	3664	3700	3722 [d]
19	$[Pt(PPh_3)_2(F_3CC{\equiv}CCF_3)]$	CD_2Cl_2	−4576	−4645 [d]	2202	3586	3566	3595 [d]
20	$[Pt(PPh_3)_2(PhC{\equiv}CCN)]$	CD_2Cl_2	−4549	−4640 [d]	1919	3430	3298	3336 [d]
			-	-	2506	3754	3855	3772 [d]
21	$[Pt(PPh_3)_2(F_3CH_2CO_2CC{\equiv}CCO_2CH_2CF_3)]$	CD_2Cl_2	−4488	−4626 [d]	2346	3665	3703	3726 [d]
22	$[Pt(PPh_3)_2(MeC{\equiv}CCN)]$	CD_2Cl_2	−4590	−4598 [d]	1923	3433	3302	3303 [d]
			-	-	2550	3778	3896	3864 [d]
23	$[Pt(PPh_3)_2(HC{\equiv}CCN)]$	CD_2Cl_2	−4539	−4573 [d]	2026	3489	3400	3434 [d]
			-	-	2581	3795	3926	3887 [d]
24	$[Pt(PPh_3)_2(NCC{\equiv}CCN)]$	CD_2Cl_2	−4395	−4586 [d]	2320	3651	3678	3696 [d]
25	$[Pt(F_3CC{\equiv}CCF_3)(PPh_3)_2]$	$CDCl_3$	−4570	−4645 [e]	2222	3597	3585	3590 [e]
26	$[Pt(F_2C{=}CF_2)(PPh_3)_2]$	$CDCl_3$	−4728	−4791 [e]	-	-	-	-
27	$[Pt(H_2C{=}CH_2)(PPh_3)_2]$	$CDCl_3$	−5033	−5065[e]	-	-	-	-
28	$[Pt(P(O\text{-}o\text{-}tolyl)_3)]$	CD_2Cl_2	−5049	−4858 [c]	-	-	-	-
29	$[Pt(PPh_3)_3]$	$THF\text{-}d_8$	−4804	−4583 [c]	2999	4025	4322	4455 [c]
30	$[Pt(dvtms)(PPh_3)]$	$CDCl_3$	−5358	−5572 [f]	2304	3643	3664	3609 [f]
	MAD/MRD (C.N. = 3)	-	120/2.6%	-	1359/37%	114/3.0%	58/1.6%	-
	MAD/MRD (All Pt(0) complexes studied)	-	107/2.3%	-	1250/34%	127/3.3%	58/1.6%	-

Experimental values obtained from: [a] Georgii et al. [12]; [b] Mann et al. [39]; [c] Benn et al. [40]; [d] Koie et al. [41]; [e] Kennedy et al. [42]; [f] Wrackmeyer et al. [43]. MAD = mean absolute deviation—$MAD = \frac{1}{n_k}\sum_{k=1}^{n_k}\left|\delta^{195}Pt_{calc.} - \delta^{195}Pt_{expt.}\right|$ MRD = mean relative deviation—$MRD = \left(\frac{1}{n_k}\sum_{k=1}^{n_k}\left|\frac{\delta^{195}Pt_{calc.} - \delta^{195}Pt_{expt.}}{\delta^{195}Pt_{expt.}}\right|\right) \times 100\%$. Model 0. Unscaled model. Model 1. $\delta^{195}Pt_{calc.} = -0.8277 \times \sigma^{195}Pt_{calc.} - 2566$. Model 2. $^{1}J^{scal.}\left(^{195}Pt - ^{31}P\right) = 0.5508 \times {}^{1}J^{calc.}\left(^{195}Pt - ^{31}P\right) + 2373.3$. Model 3. $^{1}J^{scal.}\left(^{195}Pt - ^{31}P\right) = 0.9482 \times {}^{1}J^{calc.}\left(^{195}Pt - ^{3.1}P\right) + 1478.7$.

A comparison between the calculated and experimental Pt-195 NMR chemical shift is shown in Figure 2a. Although the ranges of chemical shift within each group (C.N. 2 or 3) are small, Model 1 correctly predicted the experimental trends and proved to be very sensitive to small structural changes. Moreover, considering that one of the main applications of Pt-195 NMR in Pt(0) complexes is the determination of the stoichiometry (C.N.) of the synthesized complexes, the proposed empirical Model 1 can assist the experimentalist in this prediction.

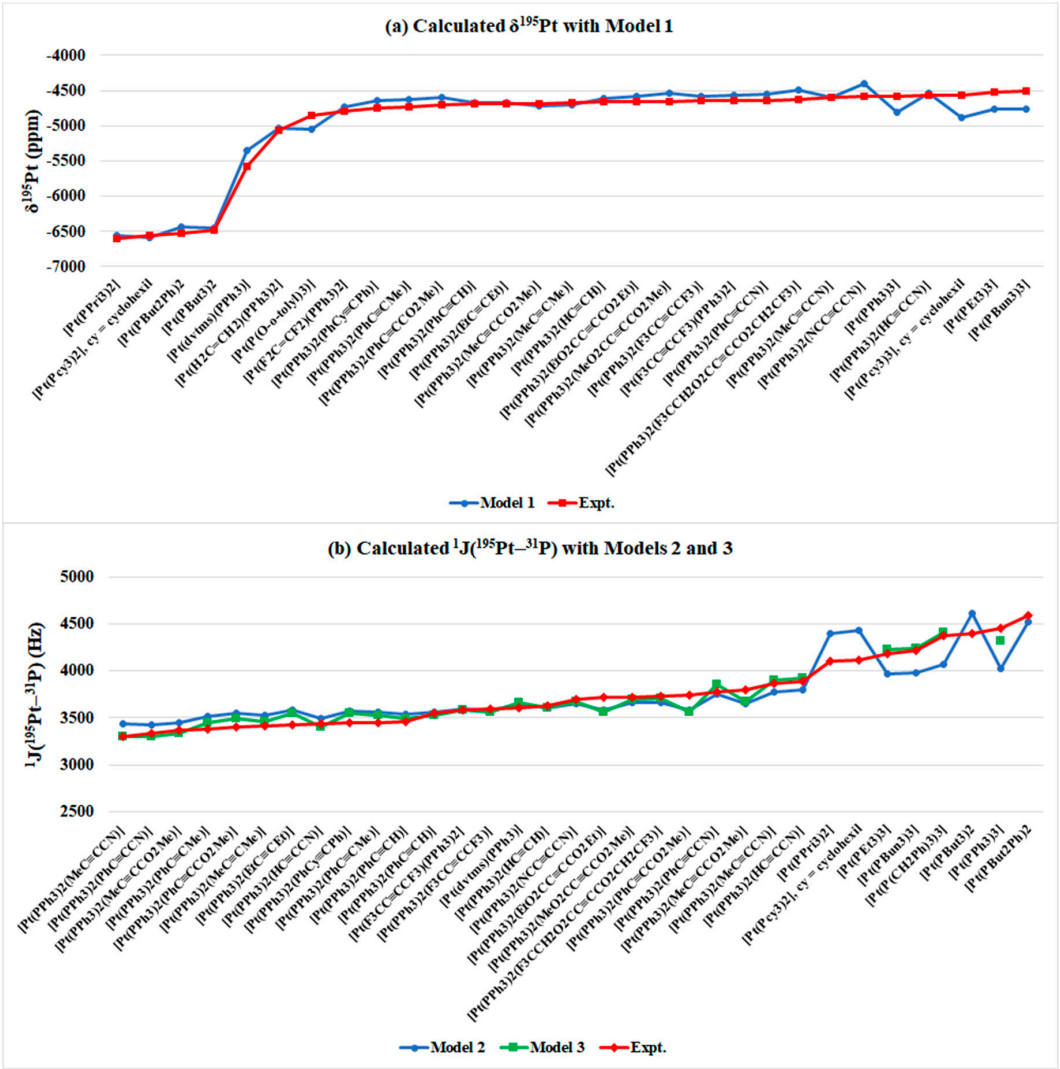

Figure 2. Relation between calculated and experimental: (**a**) δ^{195}Pt (ppm)—Model 1; (**b**) $^{1}J(^{195}Pt–^{31}P)$—Models 2 and 3.

As for the prediction of SSCC, of the 30 selected Pt(0) complexes, experimental data are available for 26 structures. Within these 26 Pt(0) complexes, a total of 33 coupling constants have been calculated. All calculated values of $^{1}J(^{195}Pt–^{31}P)$ were underestimated compared to the experimental data (Table 2), showing MAD and MRD of 1250 Hz and 34.0%, respectively (labeled as Model 0). Therefore, to correct the calculated coupling constants, a scaling procedure similar to the one used for the $^{1}J(^{195}Pt–^{15}N)$ calculation in a previous work [19] was used, Equation (2).

A linear correlation between the calculated and experimental $^{1}J(^{195}Pt–^{31}P)$ was performed for the set of 33 available coupling constants. The parameters obtained from the linear regression (Figure 1b) are listed in Table 1 (Models 2 and 3). For Model 2, which includes structures with C.N. 2 and 3, MAD and MRD were 127 Hz and 3.3%, respectively. For Model 3, which includes only C.N. 3 (29 coupling constants of the 22 complexes of

Pt(0)), MAD and MRD were 58 Hz and 1.6%, respectively, indicating excellent predictive ability of the proposed model. Comparing Models 2 and 3 with Model 0, the improvement of the results with scaling is evident. The overall MRD decreases from 34% to ~3%. Figure 2b shows a comparison between the calculated and experimental $^{1}J(^{195}Pt–^{31}P)$. From the results, it can be seen that both Model 2 and Model 3 were able to adequately predict the small variations observed experimentally in the values of the coupling constants.

In the final part of the study, the scaling Models were validated for a set of 17 Pt(0) complexes that were not included in the original set (Table 3). For this set of molecules, experimental chemical shifts are available for all 17 complexes and experimental $^{1}J(^{195}Pt–^{31}P)$ for nine complexes (18 coupling constants). For the Pt-195 NMR chemical shift, the MAD and MRD were 92 ppm and 1.7%, respectively, when Model 1 was used. For $^{1}J(^{195}Pt –^{31}P)$, MAD and MRD were 146 Hz and 3.6%, respectively, with Model 2 and 98 Hz and 2.6%, respectively, with Model 3. Both Model 2 and Model 3 were able to distinguish the coupling constants in cis- and trans-positions to the COOR group in the nine Pt(0) complexes. Despite the slightly larger error obtained for the validation group (Figure 3), the predictive capacity of the Models 1 ($\delta 1^{95}Pt$), 2, and 3 ($^{1}J(^{195}Pt–^{31}P)$) is still satisfactory and could be used to assist the experimentalists in the structural characterization.

Table 3. Calculated $\delta^{195}Pt$ in ppm, and $^{1}J(^{195}Pt–^{31}P)$ in Hz, for the Pt(0) complexes used in the validation of the proposed empirical models.

			δ^{195}Pt (ppm)		$^{1}J(^{195}Pt–^{31}P)$ (Hz)			
	Pt(0) Complexes	**Solvent**	**Model 1**	**Expt.**	**Model 0**	**Model 2**	**Model 3**	**Expt.**
	Trigonal Geometry (C.N. = 3)							
31	[Pt(ICy)(dvtms)]	$CDCl_3$	−5270	−5343 [a]	-	-	-	-
32	[Pt(Mes-NHC-Pr^n-SO_3Na)(dvtms)]	DMSO	−5212	−5352 [b]	-	-	-	-
33	[Pt(IPr-4-SO_3Na)(dvtms)]	DMSO	−5141	−5332 [b]	-	-	-	-
34	[Pt(IXy-4-SO_3Na)(dvtms)]	D_2O	−5160	−5336 [c]	-	-	-	-
35	anti-[Pt(IMes-4-SO_3Na)(dvtms)]	D_2O	−5102	−5342 [c]	-	-	-	-
36	syn-[Pt(SIMes-4-SO_3Na)(dvtms)]	D_2O	−5246	−5372 [c]	-	-	-	-
37	[Pt(Mes-NHC-Pr^n-SO_3Na)(AE)]	DMSO	−5411	−5597 [c]	-	-	-	-
38	[Pt(IXy-4,4-SO_3Na)(AE)]	DMSO	−5374	−5562 [c]	-	-	-	-
39	[Pt(PPh_3)$_2$(MeOPhHC=CHCOOPhOMe)]	Benzene	−5033	−5044 [d]	2412	3702	3766	3625 [d]
	trans/cis COOR		-	-	2797	3914	4131	4218 [d]
40	[Pt(PPh_3)$_2$(PhHC=CHCOOPhMe)]	Benzene	−4985	−5053 [d]	2502	3751	3851	3645 [d]
	trans/cis COOR		-	-	2741	3883	4077	4170 [d]
41	[Pt(PPh_3)$_2$(NO_2PhHC=CHCOOPhNO_2)]	Benzene	−5057	−5047 [d]	2408	3700	3762	3682 [d]
	trans/cis COOR		-	-	2731	3878	4068	4095 [d]
42	[Pt(PPh_3)$_2$(NO_2PhHC=CHCOOPh)]	Benzene	−5026	−5047 [d]	2505	3753	3854	3737 [d]
	trans/cis COOR		-	-	2656	3836	3997	4039 [d]
43	[Pt(PPh_3)$_2$(MePhHC=CHCOOPh)]	Benzene	−5080	−5052 [d]	2453	3724	3804	3644 [d]
	trans/cis COOR		-	-	2736	3880	4073	4207 [d]
44	[Pt(PPh_3)$_2$(PhHC=CHCOOPh)]	Benzene	−4970	−5053 [d]	2499	3750	3848	3642 [d]
	trans/cis COOR		-	-	2757	3892	4093	4176 [d]
45	[Pt(PPh_3)$_2$(NO_2PhHC=CHCOOPhOMe)]	Benzene	−5040	−5049 [d]	2495	3748	3845	3742 [d]
	trans/cis COOR		-	-	2639	3827	3981	4032 [d]
46	[Pt(PPh_3)$_2$(NO_2PhHC=CHCOOPhMe)]	Benzene	−5041	−5048 [d]	2483	3741	3833	3742 [d]
	trans/cis COOR		-	-	2644	3830	3986	4033 [d]
47	[Pt(PPh_3)$_2$(NO_2PhHC=CHCOOPr^i)]	Benzene	−5045	−5051 [d]	2513	3757	3861	3774 [d]
	trans/cis COOR		-	-	2633	3824	3975	3993 [d]
	MAD/MRD (Pt(0) complexes studied)	-	92/1.7%	-	1311/34%	146/3.6%	98/2.6%	-

Experimental values obtained from: [a] Markó et al. [10]; [b] Silbestri et al. [6]; [c] Ruiz-Varilla et al. [44]; [d] Buchner et al. [45]. MAD = mean absolute deviation—$MAD = \frac{1}{n_k}\sum_{k=1}^{n_k}\left|\delta^{195}Pt_{calc.} - \delta^{195}Pt_{expt.}\right|$ MRD = mean relative deviation—$MRD = \left(\frac{1}{n_k}\sum_{k=1}^{n_k}\left|\frac{\delta^{195}Pt_{calc.} - \delta^{195}Pt_{expt.}}{\delta^{195}Pt_{expt.}}\right|\right) \times 100\%$. Model 0. Unscaled model. Model 1. $\delta^{195}Pt_{calc.} = -0.8277 \times \sigma^{195}Pt_{calc.} - 2566$. Model 2. $^{1}J^{scal.}\left(^{195}Pt - ^{31}P\right) = 0.5508 \times {}^{1}J^{calc.}\left(^{195}Pt - ^{31}P\right) + 2373.3$. Model 3. $^{1}J^{scal.}\left(^{195}Pt - ^{31}P\right) = 0.9482 \times {}^{1}J^{calc.}\left(^{195}Pt - ^{31}P\right) + 1478.7$.

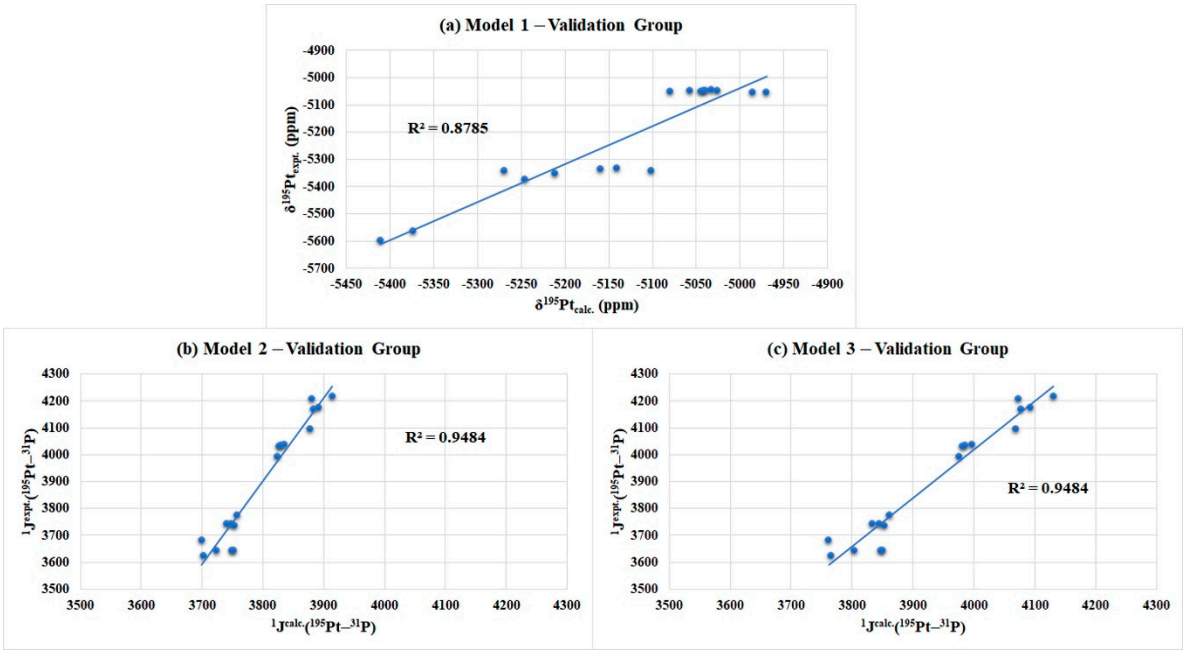

Figure 3. Correlation between the calculated and experimental values for the validation group of the models. (**a**) δ^{195}Pt for the set of 17 Pt(0) complexes (Model 1); (**b**) $^{1}J(^{195}Pt–^{31}P)$ for a set of 18 coupling constants in 9 trigonal-planar Pt(0) complexes (Model 2); and (**c**) $^{1}J(^{195}Pt–^{31}P)$ for a set of 18 coupling constants in 9 trigonal-planar Pt(0) complexes (Model 3).

Among the compounds used for validation, we highlight the Pt(0)–carbene complex ([Pt(ICy)(dvtms)], dvtms = divinyltetramethyldisiloxane (Figure 4) which is a selective and efficient hydrosilylation catalyst [10]. The calculated δ^{195}Pt was −5270 ppm, showing an absolute deviation (AD) of 73 ppm and a relative deviation (RD) of only 1.4% compared to the experimental data (δ^{195}Pt = −5343 ppm).

Structure	Calc.	Expt.	RD
Pt – C3	2.07Å	2.05Å	0.9%
Pt – C15	2.17Å	2.10Å	3.1%
Pt – C18	2.19Å	2.18Å	0.6%
Pt – C32	2.17Å	2.10Å	3.3%
Pt – C35	2.19Å	2.18Å	0.8%
C3 – Pt – C15	95.5°	91.6°	4.2%
C3 – Pt – C18	133.8°	132.3°	1.1%
C3 – Pt – C32	93.6°	91.6°	2.1%
C3 – Pt – C35	131.7°	132.3°	0.4%
C15 – Pt – C32	170.9°	174.6°	2.1%
C15 – Pt – C35	132.7°	136.1°	2.5%
C15 – Pt – C18	38.3°	40.8°	6.0%
C18 – Pt – C32	132.6°	136.1°	2.6%
C18 – Pt – C35	94.4°	95.4°	1.1%
MRD			2.2%

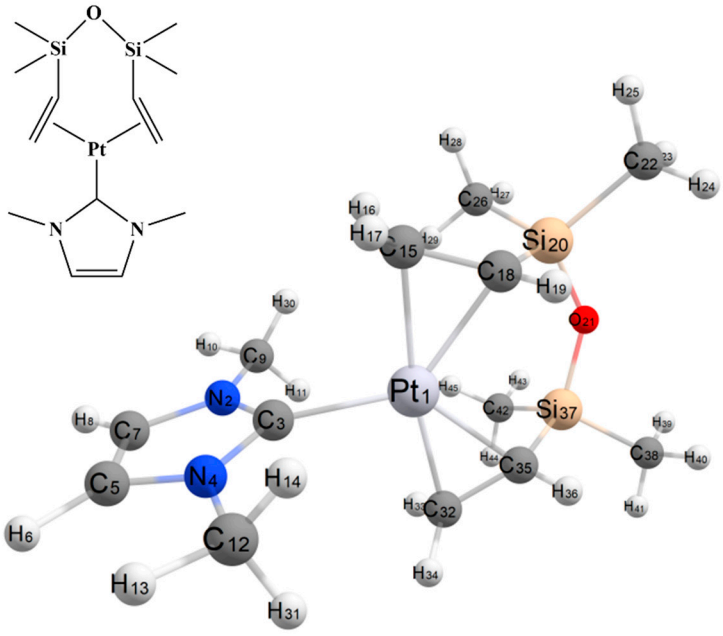

Figure 4. Pt(0)-carbene complex ([Pt(Icy)(dvtms)].

4. Conclusions

In this study, quantum mechanics computational schemes have been proposed for predicting Pt-195 NMR chemical shift and spin–spin coupling constant $^{1}J(^{195}Pt–^{31}P)$ for a series of linear and trigonal-planar in Pt(0) complexes. The NMR fundamental quantities, namely the shielding constant ($\sigma^{195}Pt$) and the coupling constant ($^{1}J(^{195}Pt–^{31}P)$), were calculated at the PBE/NMR-DKH/IEF-PCM(UFF)//B3LYP/LANL2DZ/def2-SVP/IEF-PCM(UFF) level and scaled using linear models. The Model 1, $\delta^{195}Pt_{calc} = -0.8277 \times \sigma^{195}Pt_{calc} - 2566$, predicted the Pt-195 NMR chemical shift with MAD and MRD of 107 ppm and 2.3%, respectively, for a set of 30 Pt(0) complexes with C.N. 2 and 3. For the coupling constant, Model 2, $^{1}J^{scal.}\left(^{195}Pt - ^{31}P\right) = 0.5508 \times {}^{1}J^{calc.}\left(^{195}Pt - ^{31}P\right) + 2373.3$, predicted $^{1}J(^{195}Pt–^{31}P)$ with MAD and MRD of 127 Hz and 3.3%, respectively, for a set of 33 coupling constants in 26 Pt(0) complexes. When only C.N. 3 is considered, Model 3, $^{1}J^{scal.}\left(^{195}Pt - ^{31}P\right) = 0.9482 \times {}^{1}J^{calc.}\left(^{195}Pt - ^{31}P\right) + 1478.7$, was better than Model 2, with MAD and MRD of 58 Hz and 1.6% for a set of 29 coupling constants in 22 trigonal Pt(0) complexes. We validated all Models for a set of 17 Pt(0) complexes that were not included in the original set. The results were (MAD/MRD): 92 ppm/1.7% (Model 1), 146 Hz/3.6% (Model 2) and 98 Hz/2.6% (Model 3).

In summary, the scaling models proposed here could be useful methods for predicting Pt-195 NMR parameters in Pt(0) complexes. This extends our previous protocols for predicting similar properties for Pt(II) complexes using the same quantum mechanical theory to calculate the fundamental quantities. In addition, the present results also support the use of the NMR-DKH basis set, specifically constructed for the calculation of NMR spectra of heavy metal complexes, in particular Pt complexes.

Supplementary Materials: The following are available online at https://www.mdpi.com/article/10.3390/magnetochemistry7110148/s1, The xyz coordinates of the optimized geometries of 47 Pt(0) complexes studied in the present paper are in the Supplementary Materials.

Author Contributions: Conceptualization, J.H.C.e.S., H.F.D.S., and D.F.S.P.; Methodology, J.C.H.e.S., H.F.D.S. and D.F.S.P.; Software, J.C.H.e.S., H.F.D.S. and D.F.S.P.; Validation, D.F.S.P.; Formal Analysis, J.H.C.e.S., H.F.D.S. and D.F.S.P.; Investigation, J.H.C.e.S., H.F.D.S. and D.F.S.P.; Resources, H.F.D.S. and D.F.S.P.; Writing, J.H.C.e.S., H.F.D.S. and D.F.S.P.; Supervision, H.F.D.S. and D.F.S.P.; Project Administration, D.F.S.P. All authors have read and agreed to the published version of the manuscript.

Funding: The authors would like to thank the Brazilian agency FAPERJ (E-26/201.737/2017—BOLSA and E-26/010.002261/2019—EMERGENTES) for the financial support. This study was financed in part by the Coordenação de Aperfeiçoamento de Pessoal de Nível Superior—Brasil (CAPES)—Finance Code 001.

Institutional Review Board Statement: Not applicable.

Informed Consent Statement: Not applicable.

Acknowledgments: DFSP thanks the FAPERJ for supporting to the NQTCM laboratory. HFDS thanks the FAPEMIG and CNPq for continuing support to the NEQC laboratory.

Conflicts of Interest: The authors declare no conflict of interest.

References

1. Dilruba, S.; Kalayda, G.V. Platinum-Based Drugs: Past, Present and Future. *Cancer Chemother. Pharmacol.* **2016**, *77*, 1103–1124. [CrossRef]
2. Deo, K.M.; Ang, D.L.; McGhie, B.; Rajamanickam, A.; Dhiman, A.; Khoury, A.; Holland, J.; Bjelosevic, A.; Pages, B.; Gordon, C.; et al. Platinum Coordination Compounds with Potent Anticancer Activity. *Coord. Chem. Rev.* **2018**, *375*, 148–163. [CrossRef]
3. Dedieu, A. Theoretical Studies in Palladium and Platinum Molecular Chemistry. *Chem. Rev.* **2000**, *100*, 543–600. [CrossRef]
4. Li, C.-J.; Chen, L. Organic Chemistry in Water. *Chem. Soc. Rev.* **2006**, *35*, 68–82. [CrossRef]
5. Li, C.-J. Organic Reactions in Aqueous Media with a Focus on Carbon−Carbon Bond Formations: A Decade Update. *Chem. Rev.* **2005**, *105*, 3095–3166. [CrossRef] [PubMed]
6. Silbestri, G.F.; Flores, J.C.; de Jesús, E. Water-Soluble N-Heterocyclic Carbene Platinum(0) Complexes: Recyclable Catalysts for the Hydrosilylation of Alkynes in Water at Room Temperature. *Organometallics* **2012**, *31*, 3355–3360. [CrossRef]

7. Nakajima, Y.; Shimada, S. Hydrosilylation Reaction of Olefins: Recent Advances and Perspectives. *RSC Adv.* **2015**, *5*, 20603–20616. [CrossRef]
8. Sprengers, J.W.; de Greef, M.; Duin, M.A.; Elsevier, C.J. Stable Platinum(0) Catalysts for Catalytic Hydrosilylation of Styrene and Synthesis of [Pt(Ar-Bian)(H2-Alkene)] Complexes. *Eur. J. Inorg. Chem.* **2003**, *2003*, 3811–3819. [CrossRef]
9. Troegel, D.; Stohrer, J. Recent Advances and Actual Challenges in Late Transition Metal Catalyzed Hydrosilylation of Olefins from an Industrial Point of View. *Coord. Chem. Rev.* **2011**, *255*, 1440–1459. [CrossRef]
10. Markó, I.E.; Stérin, S.; Buisine, O.; Mignani, G.; Branlard, P.; Tinant, B.; Declercq, J.-P. Selective and Efficient Platinum(0)-Carbene Complexes As Hydrosilylation Catalysts. *Science* **2002**, *298*, 204–206. [CrossRef]
11. Pregosin, P.S. Platinum NMR Spectroscopy. *Annu. Rep. NMR Spectrosc.* **1986**, *17*, 285–349. [CrossRef]
12. Georgii, I.; Mann, B.E.; Taylor, B.F.; Musco, A. ^{195}Pt n.m.r. Spectra of Some [$Pt(PR_3)_n$] Complexes. *Inorg. Chim. Acta* **1984**, *86*, L81–L82. [CrossRef]
13. Still, B.M.; Kumar, P.G.A.; Aldrich-Wright, J.R.; Price, W.S. ^{195}Pt NMR—Theory and Application. *Chem. Soc. Rev.* **2007**, *36*, 665–686. [CrossRef]
14. Pregosin, P.S. Platinum-195 Nuclear Magnetic Resonance. *Coord. Chem. Rev.* **1982**, *44*, 247–291. [CrossRef]
15. Priqueler, J.R.L.; Butler, I.S.; Rochon, F.D. An Overview of ^{195}Pt Nuclear Magnetic Resonance Spectroscopy. *Appl. Spectrosc. Rev.* **2006**, *41*, 185–226. [CrossRef]
16. Vaara, J. Theory and Computation of Nuclear Magnetic Resonance Parameters. *Phys. Chem. Chem. Phys.* **2007**, *9*, 5399. [CrossRef] [PubMed]
17. Bühl, M.; Kaupp, M.; Malkina, O.L.; Malkin, V.G. The DFT Route to NMR Chemical Shifts. *J. Comput. Chem.* **1999**, *20*, 91–105. [CrossRef]
18. Paschoal, D.; Guerra, C.F.; de Oliveira, M.A.L.; Ramalho, T.C.; dos Santos, H.F. Predicting Pt-195 NMR Chemical Shift Using New Relativistic All-Electron Basis Set. *J. Comput. Chem.* **2016**, *37*, 2360–2373. [CrossRef]
19. Carvalho, J.; Paschoal, D.; Fonseca Guerra, C.; dos Santos, H.F. Nonrelativistic Protocol for Calculating the ^{1}J(^{195}Pt-^{15}N) Coupling Constant in Pt(II)-Complexes Using All-Electron Gaussian Basis-Set. *Chem. Phys. Lett.* **2020**, *745*, 137279. [CrossRef]
20. da Silva Paschoal, D.F.; da Silva Gomes, M.; Machado, L.P.N.; dos Santos, H.F. Basis Sets for Heavy Atoms. In *Basis Sets in Computational Chemistry. Lecture Notes in Chemistry*; Perlt, E., Ed.; Springer: Cham, Switzerland, 2021; Volume 107, pp. 183–214.
21. Semenov, V.A.; Samultsev, D.O.; Rusakova, I.L.; Krivdin, L.B. Computational Multinuclear NMR of Platinum Complexes: A Relativistic Four-Component Study. *J. Phys. Chem. A* **2019**, *123*, 4908–4920. [CrossRef]
22. Sterzel, M.; Autschbach, J. Toward an Accurate Determination of ^{195}Pt Chemical Shifts by Density Functional Computations: The Importance of Unspecific Solvent Effects and the Dependence of Pt Magnetic Shielding Constants on Structural Parameters. *Inorg. Chem.* **2006**, *45*, 3316–3324. [CrossRef] [PubMed]
23. Semenov, V.A.; Rusakov, Y.Y.; Samultsev, D.O.; Krivdin, L.B. Geometries and NMR Properties of Cisplatin and Transplatin Revisited at the Four-Component Relativistic Level. *Mendeleev Commun.* **2019**, *29*, 315–317. [CrossRef]
24. Sutter, K.; Truflandier, L.A.; Autschbach, J. NMR J-Coupling Constants in Cisplatin Derivatives Studied by Molecular Dynamics and Relativistic DFT. *ChemPhysChem* **2011**, *12*, 1448–1455. [CrossRef] [PubMed]
25. Tsipis, A.C.; Karapetsas, I.N. Accurate Prediction of ^{195}Pt NMR Chemical Shifts for a Series of Pt(II) and Pt(IV) Antitumor Agents by a Non-Relativistic DFT Computational Protocol. *Dalton Trans.* **2014**, *43*, 5409–5426. [CrossRef] [PubMed]
26. Gilbert, T.M.; Ziegler, T. Prediction of 195 Pt NMR Chemical Shifts by Density Functional Theory Computations: The Importance of Magnetic Coupling and Relativistic Effects in Explaining Trends. *J. Phys. Chem. A* **1999**, *103*, 7535–7543. [CrossRef]
27. Berkefeld, A.; Reimann, M.; Hörner, G.; Kaupp, M.; Schubert, H. C–P vs C–H Bond Cleavage of Triphenylphosphine at Platinum(0): Mechanism of Formation, Reactivity, Redox Chemistry, and NMR Chemical Shift Calculations of a μ-Phosphanido Diplatinum(II) Platform. *Organometallics* **2020**, *39*, 443–452. [CrossRef]
28. Becke, A.D. Density-functional Thermochemistry. III. The Role of Exact Exchange. *J. Chem. Phys.* **1993**, *98*, 5648–5652. [CrossRef]
29. Lee, C.; Yang, W.; Parr, R.G. Development of the Colle-Salvetti Correlation-Energy Formula into a Functional of the Electron Density. *Phys. Rev. B* **1988**, *37*, 785–789. [CrossRef]
30. Stephens, P.J.; Devlin, F.J.; Chabalowski, C.F.; Frisch, M.J. Ab Initio Calculation of Vibrational Absorption and Circular Dichroism Spectra Using Density Functional Force Fields. *J. Phys. Chem.* **1994**, *98*, 11623–11627. [CrossRef]
31. Hay, P.J.; Wadt, W.R. Ab Initio Effective Core Potentials for Molecular Calculations. Potentials for the Transition Metal Atoms Sc to Hg. *J. Chem. Phys.* **1985**, *82*, 270–283. [CrossRef]
32. Hay, P.J.; Wadt, W.R. Ab Initio Effective Core Potentials for Molecular Calculations. Potentials for K to Au Including the Outermost Core Orbitals. *J. Chem. Phys.* **1985**, *82*, 299–310. [CrossRef]
33. Weigend, F.; Ahlrichs, R. Balanced Basis Sets of Split Valence, Triple Zeta Valence and Quadruple Zeta Valence Quality for H to Rn: Design and Assessment of Accuracy. *Phys. Chem. Chem. Phys.* **2005**, *7*, 3297. [CrossRef] [PubMed]
34. Scalmani, G.; Frisch, M.J. Continuous Surface Charge Polarizable Continuum Models of Solvation. I. General Formalism. *J. Chem. Phys.* **2010**, *132*, 114110. [CrossRef] [PubMed]
35. Cheeseman, J.R.; Trucks, G.W.; Keith, T.A.; Frisch, M.J. A Comparison of Models for Calculating Nuclear Magnetic Resonance Shielding Tensors. *J. Chem. Phys.* **1996**, *104*, 5497–5509. [CrossRef]
36. Wolinski, K.; Hinton, J.F.; Pulay, P. Efficient Implementation of the Gauge-Independent Atomic Orbital Method for NMR Chemical Shift Calculations. *J. Am. Chem. Soc.* **1990**, *112*, 8251–8260. [CrossRef]

37. Perdew, J.P.; Burke, K.; Ernzerhof, M. Generalized Gradient Approximation Made Simple. *Phys. Rev. Lett* **1997**, *77*, 3865. [CrossRef]
38. Frisch, M.J.; Trucks, G.W.; Schlegel, H.B.; Scuseria, G.E.; Robb, M.A.; Cheeseman, J.R.; Scalmani, G.; Barone, V.; Mennucci, B.; Petersson, G.A.; et al. Gaussian ∼09 Revision D.01. Available online: https://www.scienceopen.com/document?vid=839f33cc-9114-4a55-8f1a-3f1520324ef5 (accessed on 20 September 2021).
39. Mann, B.E.; Musco, A. A ^{31}P Nuclear Magnetic Resonance Investigation of the Structure, Equilibria, and Kinetics of [Pt(PR_3)$_n$] in Solution. *J. Chem. Soc. Dalton Trans.* **1980**, 776–785. [CrossRef]
40. Benn, R.; Michael Büch, H.; Reinhardt, R.-D. Heavy Metal Spin- $\frac{1}{2}$ Nuclei. Platinum-195 Relaxation Times in Phosphorus-Platinum(0) Compounds and Their Dependence on the Geometry of the Complex. *Magn. Reson. Chem.* **1985**, *23*, 559–564. [CrossRef]
41. Koie, Y.; Shinoda, S.; Saito, Y. Platinum-195 Nuclear Magnetic Resonance Study of Platinum(0) Complexes Containing a Series of Acetylenes. *J. Chem. Soc. Dalton Trans.* **1981**, 1082–1088. [CrossRef]
42. Kennedy, J.D.; McFarlane, W.; Puddephatt, R.J.; Thompson, P.J. Magnetic Double-Resonance Studies of Platinum-195 Chemical Shifts in Organoplatinum Compounds. *J. Chem. Soc. Dalton Trans.* **1976**, 874–879. [CrossRef]
43. Wrackmeyer, B.; Klimkina, E.V.; Schmalz, T.; Milius, W. Synthesis, NMR Spectroscopic Characterization and Structure of a Divinyldisilazane-(Triphenylphosphine)Platinum(0) Complex: Observation of Isotope-Induced Chemical Shifts 1Δ12/13C(195Pt). *Magn. Reson. Chem.* **2013**, *51*, 283–291. [CrossRef] [PubMed]
44. Ruiz-Varilla, A.M.; Baquero, E.A.; Silbestri, G.F.; Gonzalez-Arellano, C.; de Jesús, E.; Flores, J.C. Synthesis and Behavior of Novel Sulfonated Water-Soluble N-Heterocyclic Carbene (η4-Diene) Platinum(0) Complexes. *Dalton Trans.* **2015**, *44*, 18360–18369. [CrossRef] [PubMed]
45. Buchner, M.R.; Bechlars, B.; Wahl, B.; Ruhland, K. Influence of Electronically and Sterically Tunable Cinnamate Ligands on the Spectroscopic Properties and Reactivity of Bis(Triphenylphosphine)Platinum(0) Olefin Complexes. *Organometallics* **2013**, *32*, 1643–1653. [CrossRef]